

Article

Shift-Peristrophic Multiplexing for High Density Holographic Data Storage

Zenta Ushiyama, Hiroyuki Kurata, Yu Tsukamoto, Shuhei Yoshida and Manabu Yamamoto *

Department of Applied Electronics, Tokyo University of Science, 6-3-1, Niijuku, Katsushika-ku, Tokyo 125-8585, Japan; E-Mails: zetyco@xpost.plala.or.jp(Z.U.); h.kurata1109@gmail.com (H.K.); j8113631@ed.tus.ac.jp (Y.T.); syoshida@rs.tus.ac.jp (S.Y.)

* Author to whom correspondence should be addressed; E-Mail: ymanabu@te.noda.tus.ac.jp; Tel.: +81-3-5876-1437; Fax: +81-3-5876-1639.

Received: 21 November 2013; in revised form: 5 March 2014 / Accepted: 17 March 2014 /

Published: 31 March 2014

Abstract: Holographic data storage is a promising technology that provides very large data storage capacity, and the multiplexing method plays a significant role in increasing this capacity. Various multiplexing methods have been previously researched. In the present study, we propose a shift-peristrophic multiplexing technique that uses spherical reference waves, and experimentally verify that this method efficiently increases the data capacity. In the proposed method, a series of holograms is recorded with shift multiplexing, in which the recording material is rotated with its axis perpendicular to the material's surface. By iterating this procedure, multiplicity is shown to improve. This method achieves more than 1 Tbits/inch² data density recording. Furthermore, a capacity increase of several TB per disk is expected by maximizing the recording medium performance.

Keywords: holographic data storage; shift multiplexing; spherical wave; peristrophic

1. Introduction

Holographic data storage (HDS) has been researched as a next-generation mass optical storage solution [1–3]. With HDS, information is recorded as a volume hologram in thick photopolymer media. Therefore, it can achieve a higher storage capacity than that of conventional planar optical disks. As a recording medium, photopolymer material is preferred [4–6] for the following reasons: (1) it is suitable for recording a thick phase-type hologram; (2) it has potential to achieve high diffraction efficiency with

low noise, such as scattering; (3) the spectral sensitivity of the medium can be selected with comparative freedom; and (4) deterioration in the hologram does not easily occur. Issues associated with using photopolymer material, such as recording sensitivity and reliability, have been greatly improved, and this medium is currently expected to become a practical medium for HDS applications.

HDS with photopolymer media is promising for archival storage. A reduction in power consumption is an expected requirement, although hard-disk drive (HDD) technology with relatively high power requirements is currently used for archival storage in data centers. If HDS replaces HDD as an archival storage solution, a reduction in power consumption of at least 40% is expected. Considering the progress of magnetic tape or hard-disk technologies used for archival storage, the capacity required by HDS is expected to be 1–10 TB/disk in the near future. These trends indicate that improvement of the recording and reproduction methods of HDS will be required in the future; photopolymer media represents an opportunity to achieve such high-capacity storage.

The multiplexing method plays a key role in determining storage capacity, and numerous multiplexing methods have been previously proposed. Such methods can be classified roughly into Bragg-based and other techniques [3]. Bragg-based methods include angle [7–9], wavelength [10,11], phase-code [12,13], peristrophic [14–16], shift [17,18], and correlation multiplexing [2]. These methods depend on the effect of Bragg selectivity, which is determined by calculating the thickness of the medium and the wavelength and geometry of the optical system. Multiplexing methods based on other principles include polytopic [19] and aperture multiplexing [20], which are based on conservation of momentum and optical correlation.

In the present study, we examine the potential of achieving high recording density in the recording and reproduction method by combining peristrophic multiplexing and shift multiplexing with spherical reference waves [21]. In the latter method, multiplex recording is enabled simply by displacing the recording medium. However, results of our previous research indicated that the insensitivity of shift selectivity in the radial, or y -axis, direction becomes an obstruction factor to high-density recording; however, shift selectivity in the track direction and that vertical to the medium direction, or z -axis, were sensitive [22,23]. Thus, it became necessary to enhance shift multiplexing to achieve the target storage capacity by combining it with a peristrophic-multiplexing method that changes the direction of the hologram transportation wave and provides multiple records.

2. Recording Method

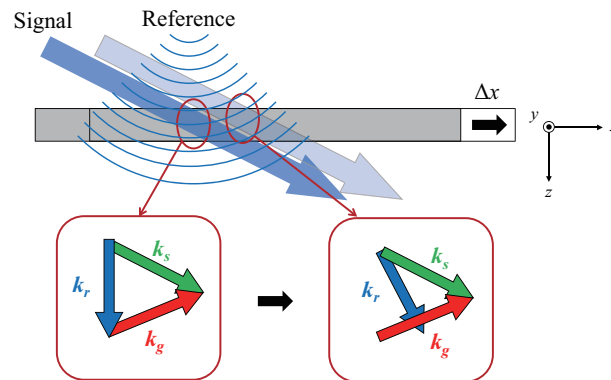
In this section, we describe our proposed shift-peristrophic multiplexing method. Figure 1 shows the conceptual illustration of shift multiplexing with spherical reference waves. In the figure, k_s , k_r , and k_g are signal, reference, and grating vectors, respectively.

Because spherical waves can be expressed as superimposed plane waves advancing in various directions, the shape of the grating varies by location. Therefore, multiplexing is enabled simply by displacing the medium. The required shift amount in the x -direction to suppress crosstalk Δx can be expressed as [21]:

$$\Delta x = \frac{\lambda z_0}{L \theta_s} \quad (1)$$

where z_0 is the location of the reference wave source, L is the medium thickness, and θ_s is the incident angle of the signal. In our previous studies [22,23], shift selectivity in the y -direction was determined to be inferior compared with the x - and z -directions because the y -direction is parallel to the hologram grating.

Figure 1. Principle of the peristrophic multiplexing.

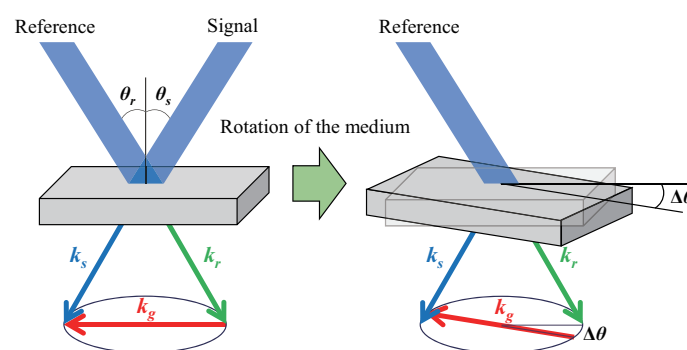


To improve the recording density by effective utilization of dynamic range, we combined shift multiplexing with spherical reference waves and peristrophic multiplexing. Figure 2 shows the principle of the peristrophic multiplexing. The relation between the wave vector of signal k_s , reference k_r , and the grating vector k_g is also shown in the figure. If the medium is rotated by a minute angle, the Bragg condition is broken by the change in each wave vector, and the recorded hologram is not reproduced. In the event that a new hologram is recorded in the current state, each hologram is independently reproduced without crosstalk. The Bragg selectivity $\Delta\theta$ of the peristrophic multiplexing with plane wave is expressed as [14]:

$$\Delta\theta = \sqrt{\frac{2\lambda}{L} \cdot \frac{\cos \theta_s}{\sin \theta_r (\sin \theta_s + \sin \theta_r)}} \quad (2)$$

where $\Delta\theta$ is the required rotation angle of the medium to suppress crosstalk, and θ_s and θ_r are the incident angles of the signal and reference, respectively.

Figure 2. Principle of the peristrophic multiplexing.



High recording density is expected using a recording method that combines such shift multiplexing with peristrophic multiplexing. The procedure of shift-peristrophic multiplexing is as follows. First,

shift multiplexing is performed along the x -direction. The medium is then rotated by $\Delta\theta$, and shift multiplexing is repeated: the procedure is shown in Figure 3. Figure 4 shows the recording method for the disk-shaped medium. An optical recording head moves in the direction of the shift multiplexing along the straight line shown in Figure 4. In addition, only the hologram diameter moves with the y -axis, and shift multiplexing is performed. The shift-multiplexed holograms are recorded at each y -axial track until the disk is full.

Figure 3. Recording method shift-peristrophic multiplexing.

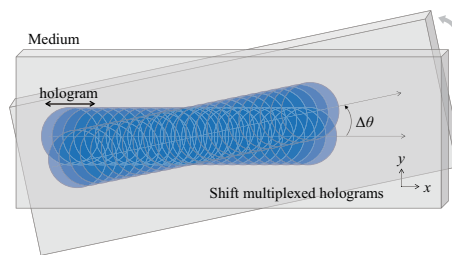
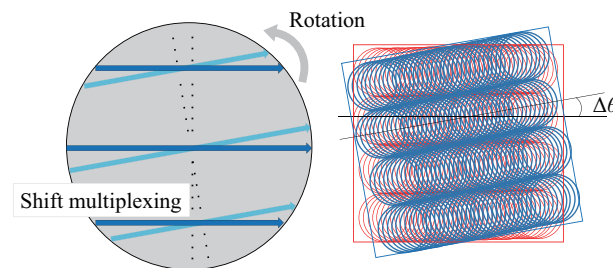


Figure 4. The recording method to the disk-shaped medium.



These holograms occupy all of the disk space by rotating the medium by 10° . This space is then overwritten with shift-multiplexed holograms. This procedure is executed for each angle, resulting in a series of composite holographic images, and can be fundamentally executed 18 times at intervals of 10° . Figure 4 shows that a multiple shift also is performed along the x -axis after the medium is rotated by 10° .

3. Experimental Evaluation

We experimentally verified the practical effectiveness of shift-peristrophic multiplexing. The composition of the experimental system is shown in Figure 5. The reference beam became a spherical wave when using an objective lens and is emitted into the medium. After the spatial light modulator (SLM) modulates the signal beam and the hologram's spatial band is limited with a low-pass filter (LPF), the beam is emitted into the medium. The bandwidth of the LPF is about twice the size of the Nyquist D , and D is determined by:

$$D = \frac{f\lambda}{\Delta} \quad (3)$$

where f is the focal length of the lens for the signal beam, λ is the wavelength, and Δ is the pixel size of SLM. The over-sampling ratio of the data page is equal to three when the charge coupled device (CCD)

signal is detected. Stepping motors are used for the shift and rotation of the medium. The minimum motor steps are $1 \mu\text{m}$ for the shift and 0.005° for the rotation. Repeat accuracies are $\pm 0.5 \mu\text{m}$ for the shift and $\pm 0.02^\circ$ for the rotation, respectively. We used the radical polymerization photopolymer as a recording medium. The photopolymer film thickness was 1.5 mm. The dynamic range of the medium indicated by $M\#$ is $M\# \approx 50$. Detailed experimental conditions are shown in Table 1.

Figure 5. Experimental setup.

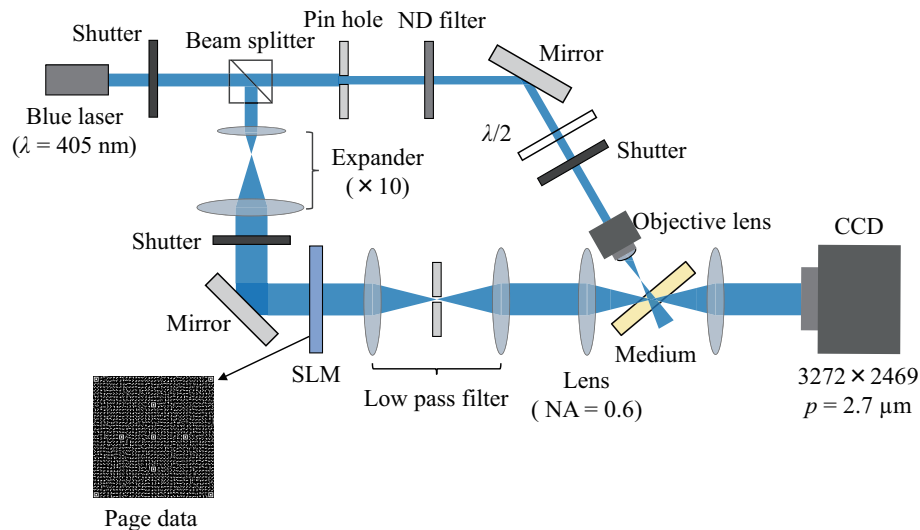


Table 1. Experimental conditions.

Wavelength λ	405 nm
Focal length f	60 mm
Medium thickness L (mm)	1.5
SLM pixel size Δ	$40 \mu\text{m}$
CCD pixel size p	$2.7 \mu\text{m}$
Incident angle of signal θ_s	45°
Incident angle of signal θ_r	15°

3.1. Evaluation of Basic Property

Figure 6 shows the results of the rotational selectivity. The horizontal axis shows the rotation angle of the medium, and vertical axis shows relative diffraction power. A single hologram is recorded, and the diffraction power is measured by rotating the medium. The numerical aperture (NA) of the objective lens for the reference beam was 0.4, 0.25, and 0 (plane wave). We determined the rotational selectivity when NA = 0.4 decreased rapidly for peristrophic multiplexing recording, in which spherical reference wave was used although the crosstalk rotation angle was 10° .

Next, we evaluated shift multiplexing with rotation. First, shift multiplexing was performed 30 times along x -direction with $50 \mu\text{m}$ intervals. After the shift multiplexing, the diffraction power of the shift-multiplexed holograms was measured (0° readout). The medium was then rotated by 10° , and the diffraction power was measured along same x -direction (10° readout). The results, shown in

Figure 7, reveal that crosstalk can be suppressed completely with 10° rotation. As a result, crosstalk did not become an issue even if a new shift-multiplexed hologram was recorded after rotating by 10° . These results were approximately the same as the rotation selectivity in peristrophic multiplexing previously obtained in this experiment.

Figure 6. Rotational selectivity.

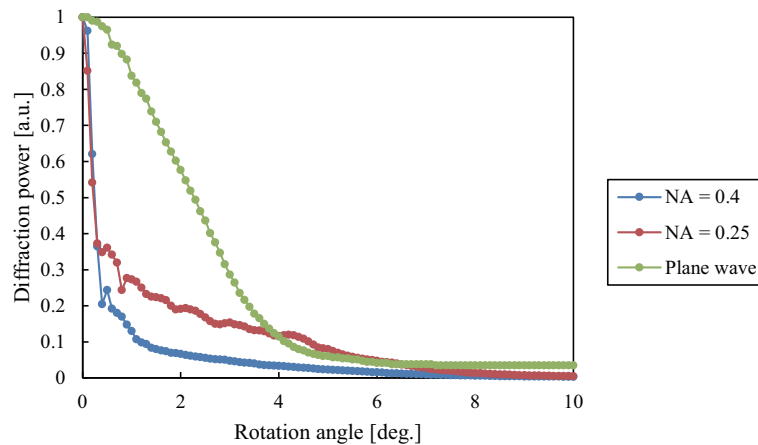
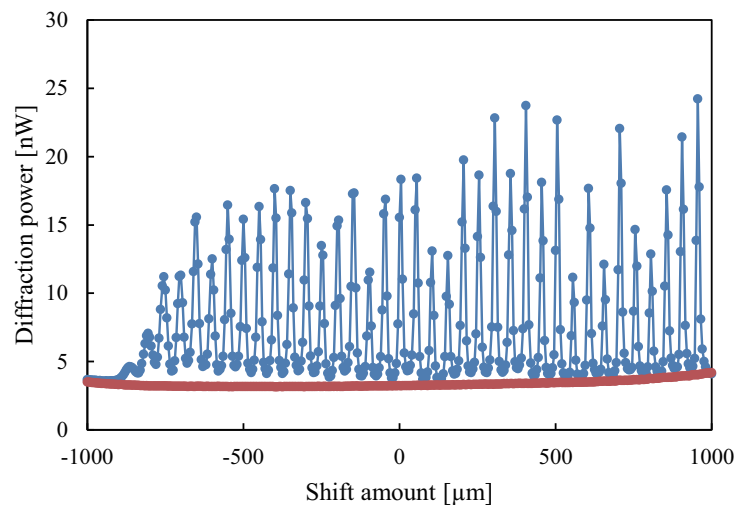
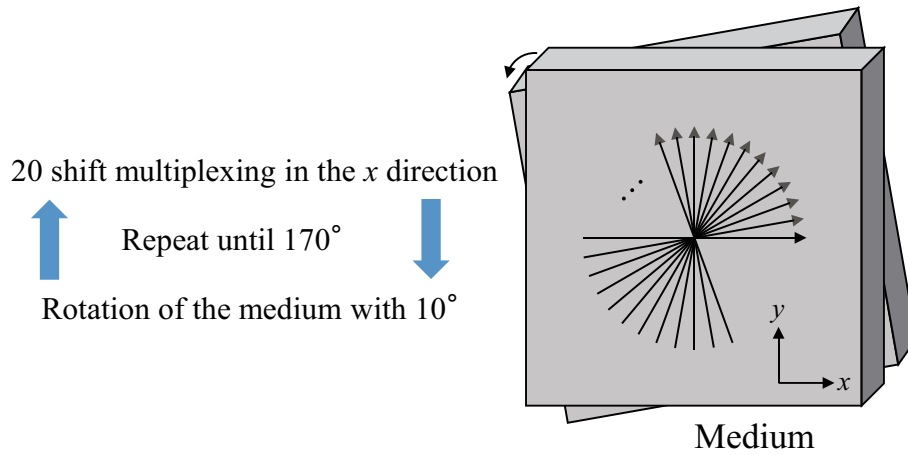
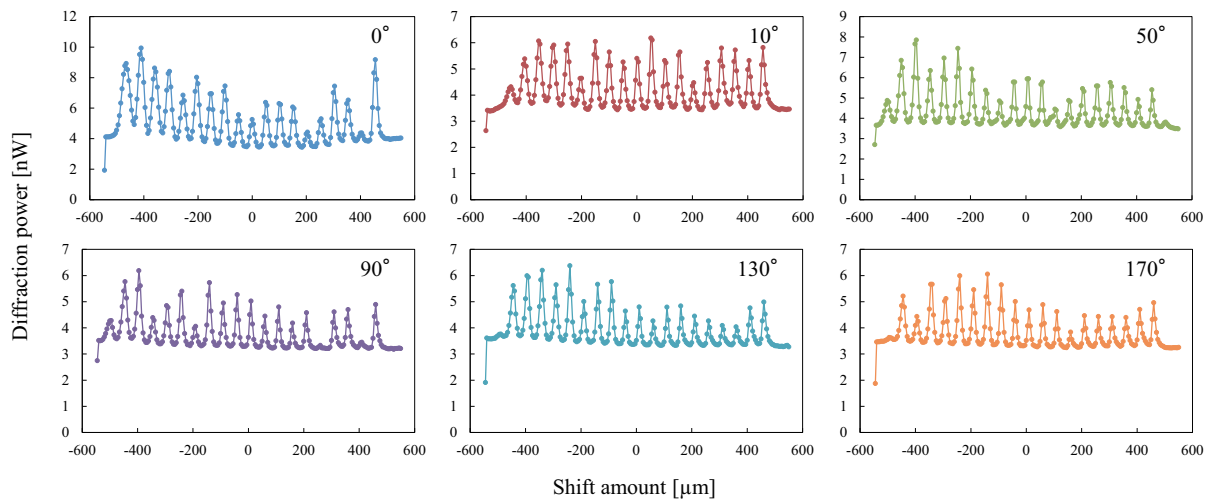


Figure 7. Rotational selectivity of shift multiplexed holograms.



3.2. Evaluation of Shift-Peristrophic Multiplexing

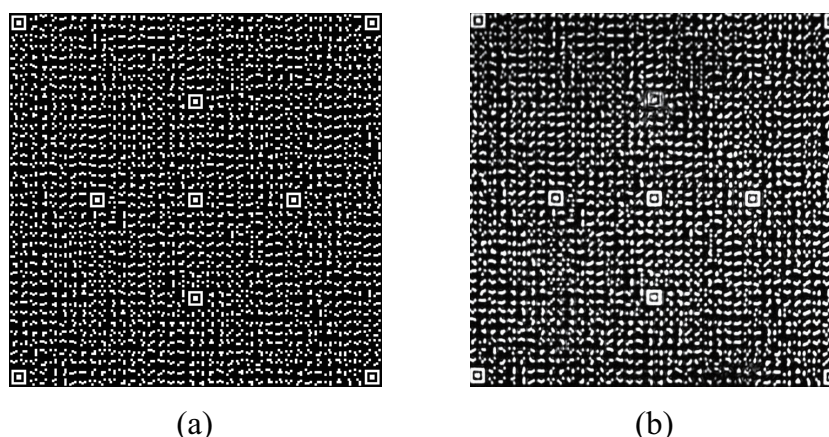
Next, we evaluated the shift-peristrophic multiplexing; the experimental methodology is shown in Figure 8. First, 20 shift multiplexing processes were performed along the x -direction with $50\ \mu\text{m}$. The medium was then rotated by 10° , 20 shift multiplexing processes were repeatedly performed up to an angle of 170° , and the diffraction power from each hologram for each rotation angle was measured. The center of rotation of the medium was always set to the center of the shift-multiplexed holograms. Figure 9 shows the diffraction power at each angle. The horizontal axis indicates the shift amount of the medium, and the vertical axis indicates the diffraction power. Multiplexing nearly 18 times was experimentally proven, and the diffraction power of the hologram changed as the multiplex number increased.

Figure 8. Experimental procedure for the shift-peristrophic multiplexing.**Figure 9.** Evaluation results of shift-peristrophic multiplexing.

A case of reproduced image obtained by this experiment is shown in Figure 10. Although the image was distorted partially its overall quality is acceptable. The signal-to-noise ratio (SNR) defined by:

$$\text{SNR} = 20 \log_{10} \frac{\mu_1 - \mu_0}{\sigma_1 + \sigma_0} \quad (4)$$

was 3.5 dB, where μ_0 and μ_1 are the average number of black and white pixels, and σ_0 and σ_1 are the standard deviations of number of black and white pixels, respectively. We obtained at least 1.5 dB from the other holograms. Therefore, it is confirmed that a relatively high multiplexing number can be achieved when recording using shift multiplexing together with peristrophic multiplexing. The optimization of the method and improvement of the medium will be studied in future research to further improve storage density.

Figure 10. Original and reproduction image. (a) Original; (b) Reproduction.

4. Conclusions

It was shown that high recording density is possible using a compound multiplexing method that combines shift multiplexing with peristrophic multiplexing. Shift multiplexing with spherical reference waves has been previously studied, and it was determined that the y -axis selectivity is inferior, thereby making high-density recording difficult. It was shown in the present study that y -axis selectivity was substantially improved by adding a peristrophic multiplexing method to enable such high recording density. In this paper, we provided fundamental proof of the effectiveness of shift-peristrophic multiplexing and the possibility of high recording density. If shift multiplexing with a $10\ \mu\text{m}$ pitch is combined with a rotation of 10° , it is possible to easily achieve $1\ \text{Tbits/inch}^2$ recording density. This possibility has been experimentally proven and will be further examined by analysis of a more practical system in the future.

Conflicts of Interest

The authors declare no conflict of interest.

References

1. Hesselink, L.; Orlov, S.S.; Bashaw, M.C. Holographic data storage systems. *Proc. IEEE* **2004**, *92*, 1231–1280.
2. Coufal, H.J.; Psaltis, D.; Sincerbos, G. *Hologr. Data Storage*; Springer: Berlin, Germany, 2000.
3. Curtis, K.; Dhar, L.; Hill, A.; Wilson, W.; Ayres, M. Materials for Holography. In *Holographic Data Storage: From Theory to Practical Systems*; Wiley: New York, NY, USA, 2010; pp. 105–132.
4. Lawrence, J.R.; O'Neill, F.T.; Sheridan, J.T. Photopolymer holographic recording material. *Optik* **2001**, *112*, 449–463.
5. Ortuño, M.; Fernández, E.; Gallego, S.; Beléndez, A.; Pascual, I. New photopolymer holographic recording material with sustainable design. *Opt. Express* **2007**, *15*, 12425–12435.

6. Zhu, J.; Wang, G.; Hao, Y.; Xie, B.; Cheng, A.Y.S. Highly sensitive and spatially resolved polyvinyl alcohol/acrylamide photopolymer for real-time holographic applications. *Opt. Express* **2010**, *18*, 18106–18112.
7. Mok, F.H. Angle-multiplexed storage of 5000 holograms in lithium niobate. *Opt. Lett.* **1993**, *18*, 915–917.
8. Staebler, D.L.; Burke, W.J.; Phillips, W.; Amodei, J.J. Multiple storage and erasure of fixed holograms in Fe-doped LiNbO₃. *Appl. Phys. Lett.* **1975**, *26*, 182–184.
9. Heanue, J.F.; Bashaw, M.C.; Hesselink, L. Volume holographic storage and retrieval of digital data. *Science* **1994**, *265*, 749–752.
10. Rakuljic, G.A.; Leyva, V.; Yariv, A. Optical data storage by using orthogonal wavelength-multiplexed volume holograms. *Opt. Lett.* **1992**, *20*, 1471–1473.
11. Campbell, S.; Yi, X.; Yeh, P. Hybrid sparse-wavelength angle-multiplexed optical data storage system. *Opt. Lett.* **1994**, *24*, 2161–2163.
12. Denz, C.; Pauliat, G.; Roosen, G. Volume hologram multiplexing using a deterministic phase encoding method. *Opt. Commun.* **1991**, *85*, 171–176.
13. Heanue, J.F.; Bashaw, M.C.; Hesselink, L. Recall of linear combinations of stored data pages based on phase-code multiplexing in volume holography. *Opt. Lett.* **1994**, *19*, 1079–1081.
14. Curtis, K.; Pu, A.; Psaltis, D. Method for holographic storage using peristrophic multiplexing. *Opt. Lett.* **1994**, *19*, 993–994.
15. Fernández, E.; García, C.; Pascual, I.; Ortuño, M.; Gallego, S.; Beléndez, A. Optimization of a thick polyvinyl alcohol-acrylamide photopolymer for data storage using a combination of angular and peristrophic holographic multiplexing. *Appl. Opt.* **2006**, *45*, 7661–7666.
16. Fernández, E.; Ortuño, M.; Gallego, S.; García, C.; Beléndez, A.; Pascual, I. Comparison of peristrophic multiplexing and a combination of angular and peristrophic holographic multiplexing in a thick PVA/acrylamide photopolymer for data storage. *Appl. Opt.* **2007**, *46*, 5368–5373.
17. Psaltis, D.; Levene, M.; Pu, A.; Barbastathis, G.; Curtis, K. Holographic storage using shift multiplexing. *Opt. Lett.* **1995**, *20*, 782–784.
18. Steckman, G.J.; Pu, A.; Psaltis, D. Storage density of shift-multiplexed holographic memory. *Appl. Opt.* **2001**, *40*, 3387–3394.
19. Anderson, K.; Curtis, K. Polytopic multiplexing. *Opt. Lett.* **2004**, *29*, 1402–1404.
20. Jang, J.; Shin, D.; Park, Y. Holographic data storage by combined use of peristrophic, angular, and spatial multiplexing. *Opt. Eng.* **2000**, *39*, 2975–2981.
21. Barbastathis, G.; Levene, M.; Psaltis, D. Shift multiplexing with spherical reference waves. *Appl. Opt.* **1996**, *35*, 2403–2417.

22. Yoshida, S.; Kurata, H.; Ozawa, S.; Okubo, K.; Yamamoto, M.; Koga, S.; Tanaka, A. High-density holographic data storage using three-dimensional shift multiplexing with spherical reference wave. *Jpn. J. Appl. Phys.* **2013**, *52*, doi:10.7567/JJAP.52.09LD07.
23. Yoshida, S.; Matsubara, T.; Kurata, H.; Horiuchi, S.; Yamamoto, M. Multi-dimensional shift multiplexing technique with spherical reference waves. *IEICE Trans. Electron.* **2013**, *E96-C*, 1520–1524.

© 2014 by the authors; licensee MDPI, Basel, Switzerland. This article is an open access article distributed under the terms and conditions of the Creative Commons Attribution license (<http://creativecommons.org/licenses/by/3.0/>).